Materials Science and Engineering C 59 (2016) 998–1006

Contents lists available at ScienceDirect

Materials Science and Engineering C

journal homepage: www.elsevier.com/locate/msec

Effect of chemical heterogeneity of biodegradable polymers on surface energy: A static contact angle analysis of polyester model films

R. Belibel [a], T. Avramoglou [a], A. Garcia [b], C. Barbaud [a], L. Mora [a,*]

[a] INSERM U1148, Laboratory for Vascular Translational Science (LVTS), Institut Galilée, Université Paris 13, Sorbonne Paris Cité, 99 Avenue Jean-Baptiste Clément, Villetaneuse F-93430, France
[b] CNRS UPR 3407, Laboratoire des Sciences des Procédés et des Matériau, Institut Galilée, Université Paris 13, Sorbonne Paris Cité, 99 Avenue Jean-Baptiste Clément, Villetaneuse F-93430, France

ARTICLE INFO

Article history:
Received 28 March 2015
Received in revised form 10 September 2015
Accepted 2 October 2015
Available online 21 October 2015

Keywords:
Biodegradable (poly((*R*,*S*)-3,3 dimethylmalic acid) derivatives
Contact angle
Sessile drop
Surface tension
Heterogeneous surfaces

ABSTRACT

Biodegradable and bioassimilable poly((*R*,*S*)-3,3 dimethylmalic acid) (PDMMLA) derivatives were synthesized and characterized in order to develop a new coating for coronary endoprosthesis enabling the reduction of restenosis. The PDMMLA was chemically modified to form different custom groups in its side chain. Three side groups were chosen: the hexyl group for its hydrophobic nature, the carboxylic acid and alcohol groups for their acid and neutral hydrophilic character, respectively. The sessile drop method was applied to characterize the wettability of biodegradable polymer film coatings. Surface energy and components were calculated. The van Oss approach helped reach not only the dispersive and polar acid–base components of surface energy but also acid and basic components. Surface topography was quantified by atomic force microscopy (AFM) and subnanometer average values of roughness (Ra) were obtained for all the analyzed surfaces. Thus, roughness was considered to have a negligible effect on wettability measurements. In contrast, heterogeneous surfaces had to be corrected by the Cassie–Baxter equation for copolymers (10/90, 20/80 and 30/70). The impact of this correction was quantified for all the wettability parameters. Very high relative corrections (%) were found, reaching 100% for energies and 30% for contact angles.

1. Introduction

Bio-polyesters are widely recommended in biomedical applications [1] as drug carriers [2] such as poly(L-lactic acid) (PLA), poly(glycolic acid) (PGA), poly(ε-caprolactone) (PCL) [3] and poly(malic acid) (PMLA) [4–8]. These biodegradable polyesters were used either alone or as copolymers side-chains to improve their mechanical properties, hydrolysis, long-term biodegradation or biocompatibility behavior for the desired therapeutic applications (PLGA [9,10], PLMA [11–15]…). Among this class of polymers, the PMLA is known to present good biocompatibility, non-toxicity in vitro and in vivo, non-immunogenic properties and stability in the bloodstream [5,16–19]. The particularity that led us to choose this family of polyesters is the presence of functionalized groups in their side-chain which, furthermore, allow chemical modification for grafting and thus, delivering drugs [20]. The copolymers derived from PMLA studied in this work were chosen to cover a coronary stent, and thus deliver a drug.

Indeed, surface wettability of the film coatings is directly governed by their chemical composition, which is known to modulate the implant biointegration [21]. Thus, it is of importance to measure contact angles in order to calculate the values of surface free energy and its components (dispersive, polar, acid and basic) for the films coatings. Indeed, this characterization could then be used to research relationships between surface chemical composition and cell response for further studies. However, copolymer surfaces are chemically heterogeneous and wettability of non-ideal surfaces is still under consideration in literature [22,23].

Basically, it is necessary to bring correction to contact angles because the different chemical composition in amphiphilic polymers is responsible for surface energy modifications compared to ideal homogeneous surfaces. Cassie–Baxter equation is generally used to perform theses corrections [24,25]. For heterogeneous surfaces composed of two homogeneous component surfaces (labeled 1 and 2 respectively) the equation is [26]:

$$\cos\theta^* = f_1 \cos\theta_1 + f_2 \cos\theta_2 \quad (1)$$

Where θ_1, θ_2, f_1 and f_2 (with $f_1 + f_2 = 1$) are contact angles and area surface fractions respectively for each component individually. θ^* is the Cassie apparent contact angle.

Moreover, surface roughness is also a parameter that has to be taken into account when contact angles studies are undertaken because in cases where average surface roughness (Ra) is important, contact angles can be increased due to this roughness [27]. Finally, correction due to the different chemical composition was calculated and the impact of this correction on surface free energies and components (dispersive, polar (acid and basic)) values was quantified. This quantification was

* Corresponding author.
E-mail address: Laurence.mora@univ-paris13.fr (L. Mora).

http://dx.doi.org/10.1016/j.msec.2015.10.010
0928-4931/

performed as a function of the acidic percentage (AP) of the polymers chemical formulae.

The purpose of the present study was the characterization of polymer surfaces having a wide range of chemical composition by determining the contact angle, surface roughness and surface free energies and components for each sample. Therefore, this material is the poly((*R*,*S*)-3,3 dimethylmalic acid) (PDMMLA) obtained by anionic ring-opening polymerization of racemic α,α,β-trisubstituted-β-lactones as previously published [28–30].

2. Material and methods

2.1. Polymers synthesis

Amorphous PLA (M_n = 20 000 g/mol) was purchased from Sigma Aldrich (France). Anhydrous THF was distilled on sodium-benzophenone. In all other cases, the commercially available chemicals were purchased from Sigma Aldrich (France) and employed as received. All reactions, with anhydrous organic solvents were performed under nitrogen atmosphere. Synthetic PDMMLAs were prepared in anhydrous THF solution using the previously reported procedure [30]. The β-lactones monomers were synthesized according to the literature procedure as well [31]. Benzylic lactone (4-benzyloxycarbonyl-3,3-dimethyl-2-oxetanone), hexylic lactone (4-hexyloxycarbonyl-3,3-dimethyl-2-oxetanone) and benzyloxypropylic lactone (4-(3-benzyloxypropyl)carbonyl-3,3-dimethyl-2-oxetanone) were used for the synthesis of corresponding homopolymers PDMMLA-H, PDMMLA-He and PDMMLA-OH, respectively. For the synthesis of the different copolymers, only benzylic and hexylic lactones were used. Briefly, as an example for the preparation of PDMMLAH_{20}-*co*-He_{80} (20/80), 513 mg (2,9 mmol) of benzylic lactone and 2 g (8,76 mmol) of hexylic lactone were dissolved in 50 mL of anhydrous THF solution and added, to a two-neck flask containing initiator (10^{-2} equiv., 0.116 mmol, 29.26 mg) under nitrogen atmosphere. The polymerization was followed by FTIR spectroscopy analysis indicating the disappearance of the lactone band at 1850 cm^{-1} and stirred at room temperature for 24 h (100% conversion). The polymer was isolated by precipitation in ethanol and then it underwent a catalytic hydrogenolysis in presence of palladium on charcoal to obtain carboxylic acid (PDMMLA-H and PDMMLA copolymers) and alcohol (PDMMLA-OH) [30]. The polymers with 0, 10, 20, 30 and 100% of acidic groups were named as 0/100, 10/90, 20/80, 30/70 and 100/0, respectively.

2.2. Samples preparation

To obtain polymer films, the PDMMLAs were dissolved in acetone and PLA in chloroform. The polymer solution was then deposited on glass slides. After the evaporation of solvant at room temperature, glass slides were dried at 37 °C overnight in a vacuum oven. Glass is used as a reference sample.

2.3. PDMMLA polymers characterization

2.3.1. Characterization of chemical structure

FTIR spectra were recorded on AVATAR 370 TF-IR Thermo Nicolet spectrometer using Nicolet OMNI-Sampler ATR Smart Accessory (Ge, DTGS). Adsorption bands are given in cm^{-1}.

^1H and ^{13}C NMR spectra were recorded on BRUKER AM-400 MHz spectrometer using CD_3COCD_3 as solvent and with the residual solvent signals as internal standard, unless otherwise indicated. Chemical shifts were given in ppm (δ) and coupling constants in Hz. The following abbreviations were used to describe the peak pattern: s (singlet), d (doublet), t (triplet), q (quartet) and m (multiplet).

The absolute average molecular weights and molecular weight distributions were determined at room temperature by coupling online a high performance size exclusion chromatograph (HPSEC), a multi-angle laser light scattering detector (MALLS), a viscometer and a differential refractive index (dRI) detector. THF, used as carrier, was filtered through a 0.1 μm filter unit (Millipore, Billerica, USA), carefully degassed (DGU-20A3R Shimadzu, Kyoto, Japan), and eluted at a 0.5 mL/min flow rate (LC10Ai Shimadzu, Kyoto, Japan). 100 μL of a 0.2 μm-filtered sample solution (at about 20 mg/mL) were injected with an automatic injector (SIL-20A HT Shimadzu, Kyoto, Japan). The column packing was a polystyrene-divinylbenzene gel. The MALLS photometer, a miniDawn TREOS from Wyatt Technology Inc. (Santa Barbara, CA, USA) was provided with a fused silica cell and a Ga–As laser (λ = 665.8 nm). The whole collected data: light scattering (LS), dRI were analyzed using the Astra v6.0.6 software package. Molar mass were obtained with the Zimm order 1 method. The concentration of each eluted fraction was determined with dRI (RID10A Shimadzu, Kyoto, Japan) according to the measured values of dn/dc (0.05 mL/g) [32].

All glass transition (*Tg*) temperatures of different polymers were obtained using Differential Scanning Calorimetry (DSC). DSC was measured on a SDT Q600 analyzer (TA instrument, Guyancourt, France). In a typical run, polymers were first put in the furnace and heated from −60 °C to 200 °C by means of a temperature ramp of 10 °C/min. This operation was repeated twice. *Tg* was determined from the inclination point of the second heating curve.

2.3.2. Atomic force microscopy (AFM)

AFM was used to obtain topographic images of surface samples. The AFM machine was a nanoscope 5 (Bruker-Nano) and the cantilever was a Veeco tip silicon probe with aluminum reflex coating (resonant frequency: 300 kHz) and with a constant force of 40 N/m. Imaging was performed in the air, at room temperature, and using the tapping mode. Surface morphology and roughness parameters were determined by the AFM software program. The (10 μm × 10 μm) 2D images of topography were obtained with a resolution of 256_256 pixels. Surface roughness (Ra (nm)) was then evaluated from 10 μm × 10 μm (100 μm^2) images.

2.3.3. Contact angle measurements and surface free energy (SFE) calculations

Contact angles were carried out using a GBX Scientific Instrument (Romans, France). A drop of 2 μL of a chosen probe liquid was deposited on the sample surface through a syringe. The drop image was stored by a video camera and an image analysis system (Windrop++ software) calculated the contact angle (θ) from the shape of the drop. Before measurement, samples were rinsed in distilled water and dried under N_2. Contact angles were measured in the air at room temperature. For each substratum, three probe liquids (L) of different polarities were used: distilled water, formamide (Sigma Chemical CO) and diiodomethane (Sigma Chemical CO—St. Louis MO USA). For each probe liquid and surface, 10 contact angles were measured (with two separate samples) and the mean value was calculated. The total SFE (γ_{TOT}) of the different surfaces were calculated using the Van Oss model [33] which brings together the dispersive (γ_{LW}) and the polar acid–base (γ_{AB}) components. The polar acid–base (γ_{AB}) components are itself divided into two parts, acid (γ_A) and basic (γ_B).

2.3.4. Statistical analysis

The statistics used here for contact angle and AFM measurements were based on a comparison of variances and means of two populations by the Student test (t-test with Excel software). Statistical calculations were performed using n = 10 different values (two separate samples) for contact angles measurements and using n = 3 different areas (4 μm^2, 25 μm^2 and 100 μm^2 separate samples) for AFM roughness calculations. The probability of correlation was based on the Pearson coefficient (p). While *p*-value is less than 0.01, a statistically significant difference is achieved between the two populations of values that are compared.

3. Results and discussion

3.1. PDMMLA polymers synthesis

For this study, six polymers were chosen: three homopolymers and three statistical copolymers. Only copolymers are tested in selected biomedical applications in other studies (data not shown). For a closer characterization of the behavior of polymers, the homopolymers should also be studied. Since the six polymer films were deposited on glass slides and the PLA was the most used polymer for the coating of stents in recent years [34], all results in this study were also compared for each case with glass and PLA. The –COOH group in the side-chain furnishes the acid hydrophilic character for copolymers, the hexyl group brings the hydrophobic character and the –OH group provides the neutral hydrophilic character. The alcohol functions on the homopolymer chains (PDMMLA-OH named HP-OH) were often used for its opsonization phenomenon [35]. At the same time, acid hydrophilic and hexylic homopolymers (PDMMLA-H 100/0 in the present paper and PDMMLA-He labeled as 0/100, respectively) were synthesized. Three statistical copolymers with different hydrophobic/hydrophilic balance in the side-chain of copolymers were also prepared: PDMMLAH$_{10}$-*co*-He$_{90}$ named 10/90, PDMMLAH$_{20}$-*co*-He$_{80}$ named 20/80 and PDMMLAH$_{30}$-*co*-He$_{70}$ named 30/70 (Fig. 1).

These carboxylic acid ratios incorporated during the polymer synthesis (translated by "AP") were selected to vary the kinetic of hydrolysis. The degradation, regardless of carboxylic acid percentage (10, 20 and 30), was more or less slower. Since these materials will be in direct contact with blood and vascular cells, it is important to study the wettability, thermomechanical and viscoelastic properties and cell interaction behavior. Finally, we will be able to determine the appropriate PDMMLA copolymer having the best qualities to cover the metallic stent. Such an attempt is essential to overcome the limitations of the existing degradable polymers such as PLA. Despite its widespread use for medical applications, PLA exhibits frequently a limited cell response and poor interaction with body tissue and fluids [14,19,36–38]. Its major disadvantages are slow degradation, poor hydrophilicity and poor ductility (higher glass temperature (*Tg*)) which limit its applications [36,39]. Therefore, the modification of PLA surface properties has become crucial to especially meet the requirements of biomedical applications [9,11,14,40]. Unfortunately, adjusting its rate of degradation, surface wettability, functionalization and thermo-mechanical properties is somewhat deficient.

The objective of this work is to determinate the surface properties of different PDMMLA polymer films.

Synthetic PDMMLAs were successfully prepared by a living anionic ring-opening polymerization of corresponding β-lactones as monomers: benzylic lactone "R = –CH_2Ph", hexylic lactone "R = –$(CH_2)_5$–CH_3" and benzyloxypropylic lactone "R = –$(CH_2)_3$–O–CH_2Ph" in anhydrous THF solution using the previously reported procedure (Scheme 1) [30]. PDMMLA statistical copolyesters were prepared from two different racemic β-lactones (benzylic and hexylic lactones). The latter were chosen because they bring the hydrophilic and hydrophobic characters to these copolymers. The tetraethylammonium benzoate was used as initiator (Scheme 1).

3.2. Polymer characterization

3.2.1. Characterization of polymers chemical structure

The different polymers were characterized by FTIR, ^{1}H and ^{13}C NMR, SEC and DSC. The different copolymers characteristics are given in the table. FTIR spectroscopy analysis showed the ester characteristic band at 1751 cm^{-1} and the disappearance of the lactone band at 1838 cm^{-1} for all polymers (Fig. 2).

The chemical structure of all PDMMLA polymers was confirmed by ^{1}H and ^{13}C NMR (Table 1). Therefore, signals around 5.20 and 7.38 ppm on ^{1}H NMR spectrum confirmed the presence of benzylic group and those around 0.89, 1.26 and 4.10 ppm characterized the hexylic group. In addition, signals assigned to benzyloxypropylic group are appeared at 1.93, 3.54, 4.27 and 4.49 ppm.

The co-monomers relative contents (10, 20 and 30%) were obtained by ^{1}H NMR using the integration ratio of peak at 4.15 ppm corresponding to –CH_2–O-hexyl and that at 5.20 ppm corresponding to –CH_2–O-benzyl (Fig. 3a).

Fig. 3a showed that the proportion of the benzylic and the hexylic units in the copolymer 30/70 was 30.1% and 69.9%, respectively.

After a catalytic hydrogenolysis in presence of 10% of palladium on charcoal on the polyester, it's possible to obtain carboxylic acid group (when R = –CH_2Ph) and alcohol group (when R = –$(CH_2)_3$–O–CH_2Ph) (Scheme 1). As mentioned above, these ionic and non-charged groups (carboxylic acid and alcohol, respectively) are used one hand for their hydrophilic properties and other hand for the possibility to react with bioactive or targeting molecules [28,41,42]. The hexyl group is used for their hydrophobic properties, which gives access to a wide variety of amphiphilic copolymers. Polymers catalytic hydrogenolysis was confirmed by the disappearance of benzylic peaks at 5.2 and 7.4 ppm on ^{1}H NMR spectrum for 100/0 and copolymers (Fig. 3b) and with the disappearance of benzyloxypropylic peaks at 1.93, 3.54, 4.27 and 4.49 ppm.

Glass temperature (*Tg*) of PDMMLA copolymers don't exceed 20 °C which is lower than the physiological temperature whereas PLA has a higher *Tg* (about 63 °C) having thus less ductility and softness (Table 2). These thermal properties of PDMMLA polymers present an encouraging result for applying these biomaterials to cover the cardiovascular stents.

3.2.2. Atomic force microscopy

AFM images of surfaces are shown in Fig. 4a. Roughness surface distribution appears to be more homogeneous 10/90 (0.106 ± 0.002) surface compared to the two other copolymers 20/80 (0.184 ± 0.008)

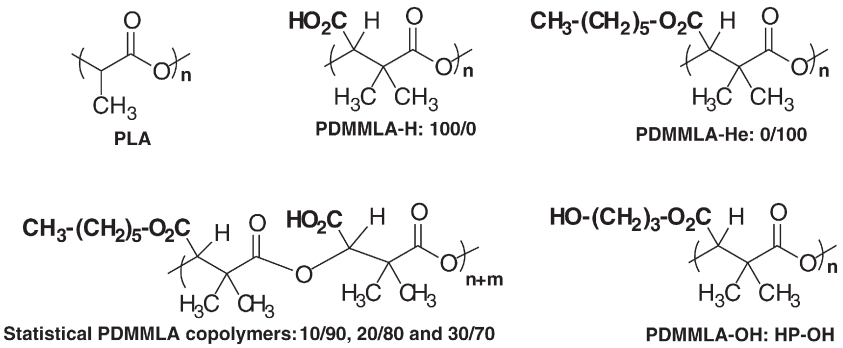

Fig. 1. Chemical structures of different studied polymers.

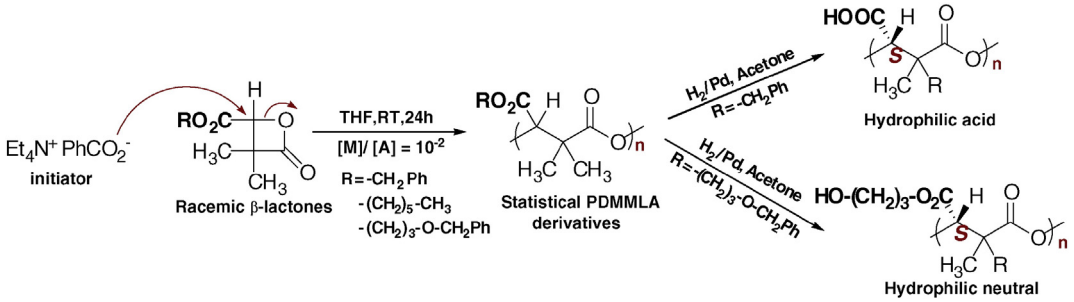

Scheme 1. Synthetic route to PDMMLA derivatives.

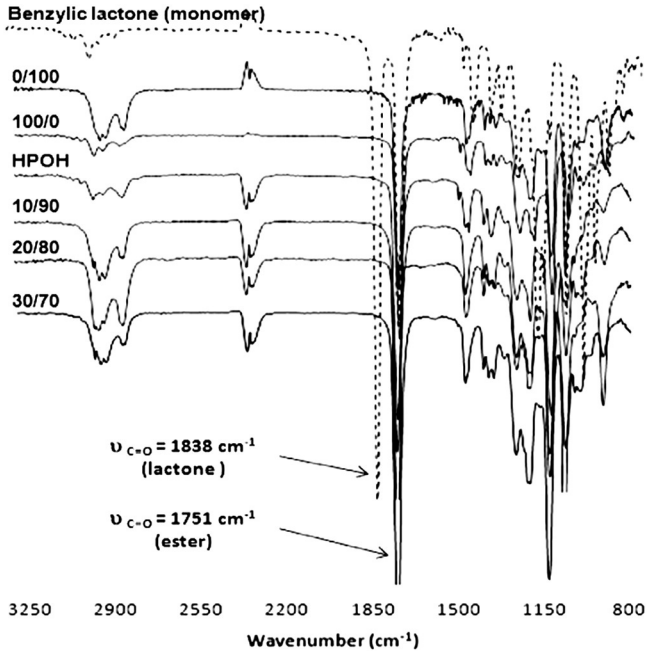

Fig. 2. FTIR spectra of the benzylic lactone monomer and PDMMLA polymers.

and 30/70 (0.216 ± 0.014). All the other surfaces, except homopolymers 0/100 (0.056 ± 0.009) and 100/0 (0.169 ± 0.014), are more heterogeneous in term of surface topography (glass (0.362 ± 0.004), PLA (0.486 ± 0.075) and HP-OH (1.112 ± 0.355)). Fig. 4b summarizes the Ra values of all the considered surfaces. Because surface roughness was on the order of nanometers, it did not affect contact angles. Also, the potential impact of surface roughness on surface energy calculation and contact angle values was considered as negligible. Thus, it was not taken into account in this paper, as in other studies [43,44]. Moreover, a statistically linear correlation ($R^2 = 0.98$, $p < 0.01$) was found between the four polymers versus AP (0/100, 10/90, 20/80 and 30/70) (Fig. 4b). For all these samples, average roughness Ra (nm) was found to be statistically different, two by two using n = 3 different values for each group. Indeed, a statistical significance difference was observed between two groups: PLA—0/100 ($p < 0.01$), 0/100—10/90 ($p < 0.001$), 10/90—20/80 ($p < 0.001$), 20/80—30/70 ($p < 0.01$), 30/70—100/0 ($p < 0.01$) and 100/0—HP-OH ($p < 0.001$). A significant difference was also obtained between "glass" and PLA, 0/100, 10/90, 20/80, 30/70, 100/0 and HP—OH ($p < 0.05$, $p < 0.0001$, $p < 0.0001$, $p < 0.001$, $p < 0.001$, $p < 0.001$ and $p < 0.001$, respectively).

3.2.3. Rough wettability

Water sessile drop contact angle values are shown in Table 3. Hydrophobicity in PDMMLA copolymers increases with the decreasing of the acidic group's percentage incorporated in the side-chain of copolymer (AP). The statistical analysis between all the samples two by two, using n = 20 different values for each group, revealed that a statistical significance difference was observed between two groups: PLA—0/100, 0/100—10/90, 10/90—20/80, 20/80—30/70, 30/70—100/0, 100/0—glass and 100/0—HP-OH ($p < 0.0001$ for all groups).

The PLA water contact angle is in accordance with the literature [45,46]. Formamide and diiodomethanne contact angle values are also shown in Table 3. They are used to calculate the total surface free energies and components (dispersive, polar (acid and basic)) for all samples.

For formamide contact angle values, a statistical analysis between all the samples two by two, using n = 20 different values for each group, gave that a statistical significant difference was observed between two groups: PLA—0/100, 0/100—10/90, 10/90—20/80, 20/80—30/70 and 30/70—100/0 ($p < 0.001$ for all groups) and no significant difference between 100/0—HP-OH group ($p > 0.05$). In the same manner, for diiodomethane contact angle values, a statistical analysis between all these samples groups indicated a significant difference, for the same couples of surfaces as just above for formamide ($p < 0.001$).

Table 1
^{1}H and ^{13}C NMR data for all PDMMLA homopolymers and copolymers.

Polymers		^{1}H NMR (δ ppm)[a]	^{13}C NMR (δ ppm)[a]
Homopolymers	0/100	0.86 (m, 3 H, $\underline{CH_3}$–CH_2), 1.26 (m, 9 H, CH_3, 3 × CH_2), 1.40 (m, 3 H, CH_3), 1.59 (m, 2 H, $\underline{CH_2}$), 4.10 (m, 2 H, CH_2–O), 5.38 (m, 1 H, CH).	14.47 ($\underline{CH_3}$–CH_2), 23.35 (CH_3), 26.34 ($\underline{CH_2}$–CH_3), 29.34 (CH_3), 32.25 (3 × CH_2), 46.03 (C), 66.29 (CH_2–O), 77.15 (CH), 168.25, 173.71 (2 × C═O).
	100/0	1.20 (m, 3 H, CH_3), 1.29 (m, 3 H, CH_3), 5.17 (m, 2 H, CH_2), 5.35 (m, 1 H, CH), 7.36 (m, 5 H, Ph).	21.54, 30.60 (2 × CH_3), 45.78 (C), 67.72 (CH_2–O), 76.83 (CH), 129.18, 129.32, 136.08, 136.17 (Ph), 167.88, 173.57 (2 × C═O).
	HPOH	1.24 (m, 6 H, 2 × CH_3), 1.93 (m, 2 H, CH_2), 3.54 (m, 2 H, CH_2–O), 4.27 (s, 2 H, CH_2–CO_2), 4.49 (s, 2 H, $\underline{CH_2}$–Ph), 5.39 (m, 1 H, CH), 7.28 (m, 5 H, Ph).	22.35 (2 × CH_3), 45.74 (C), 63.47, 63,56 (–O–$\underline{CH_2}$–CH_2–$\underline{CH_2}$–O–), 66.95 (–$\underline{CH_2}$–CH_2–O–), 73.21 ($\underline{CH_2}$–Ph), 77.01 (CH), 128.09, 128,20, 128,98, 139,56 (Ph), 168.04, 173,62 (2 × C═O).
Copolymers	10/90	0.89 (t, 3 H, $\underline{CH_3}$–CH_2), 1.31 (m, 18 H, 4 × CH_3 and 3 × CH_2), 1.64 (m, 2 H, CH_2), 4.15 (m, 2 H, CH_2–$\underline{CH_2}$–O), 5.20 (m, 2 H, Ph–$\underline{CH_2}$–O), 5.33 (m, 2 H, 2 × CH), 7.40 (m, 5 H, Ph).	14.45 ($\underline{CH_3}$–CH_2), 23.32 (2 × CH_3), 26.31 ($\underline{CH_2}$–CH_3), 29.31 (2 × CH_3), 32.22 (3 × CH_2), 45.98 (2 × C), 66.28 (CH_2–$\underline{CH_2}$–O), 67.88 (Ph–$\underline{CH_2}$–O), 77.14 (2 × CH), 129.38, 129.62, 136.45 (Ph), 168.22, 168.29, 173.68, 173.90 (4 × C═O).
	20/80		
	30/70		

[a] NMR data for all PDMMLA polymers before hydrogenolysis. ^{1}H NMR (400 MHz in CD_3COCD_3) and ^{13}C NMR (100 MHz in CD_3COCD_3).

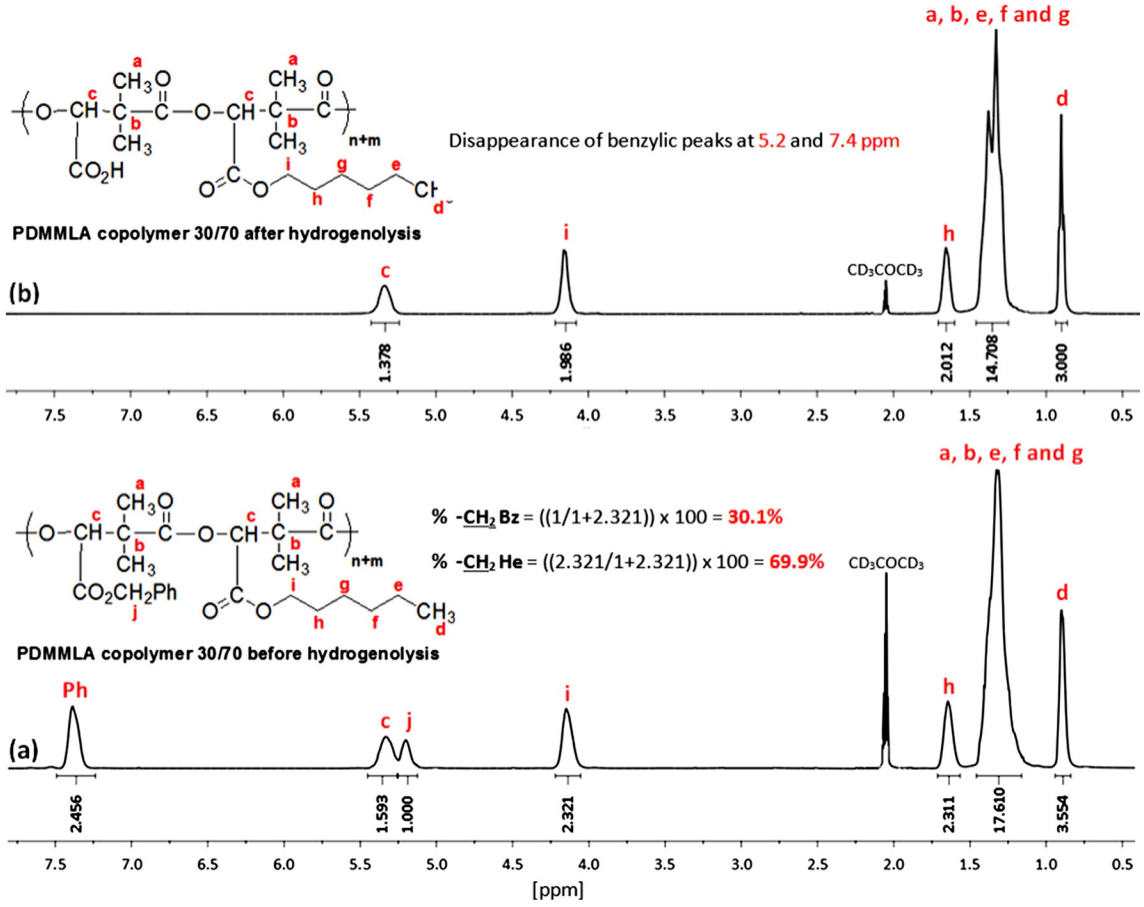

Fig. 3. ^{1}H NMR spectra of PDMMLA copolymer 30/70 (a) before hydrogenolysis and (b) after hydrogenolysis.

Fig. 5a shows the total surface free energy (γ_{TOT}) for each surface (non-Cassie corrected). Its value clearly increases with AP. It also indicates the values of non-corrected dispersive (γ_{LW}) and polar acid–base component (γ_{AB}) of the surface free energy. Polar interactions are due to Coulomb interactions between permanent dipoles but also to interactions between induced and permanent ones whereas time fluctuations in the molecules charge distribution contribute to dispersive interactions [47]. For surface free energy, dispersive and polar acid–base components, the statistical analysis between all the samples two by two (PLA—0/100, 0/100—10/90, 10/90—20/80, 20/80—30/70, 30/70—100/0, 100/0—glass and 100/0—HP-OH), using n = 20 different values for each group, revealed that a statistical significance difference was observed between all groups ($p < 0.001$ for all groups).

For all the surfaces γ_{LW} is higher than γ_{AB} due to the major presence of $-CH_2$ groups inside the polymer chains. However γ_{AB} is not negligible and is increasing regularly with AP which brings polar oxygen atoms in the structure. This correlation includes not only the chemically heterogeneous copolymers (10/90, 20/80, 30/70) but also the two homogeneous references (0/100 and 100/0). Glass exhibits a high polar component due to its oxygen atoms containing free electrons as well. This is confirmed by Fig. 5b where it can be seen that non-corrected

Table 2
Characterization of different homopolymers and copolymers.

Polymers		Copolymers composition (%)[b]		Characterization of polyesters				
		PDMMLA-H	PDMMLA-He	M_{nTh} (g/mol)[c]	M_n (g/mol)[c]	M_w (g/mol)[c]	D[c]	Tg (C°)[d]
Homopolyesters	PLA[a]	/	/	20 000	12 805	13 042	1.02	+63.4[e]
	0/100	/	/	23 400	19 789	21 283	1.07	−15.0
	100/0	/	/	22 800	29 393	30 120	1.02	+67.9
	HP-OH	/	/	29 200	19 955	20 842	1.04	+7.6
copolyesters	10/90	9.99	90.01	22 860	18 062	19 109	1.05	−14.2
	20/80	19.90	80.10	22 920	18 293	20 015	1.09	+8.2
	30/70	30.10	69.90	22 980	18 549	20 776	1.12	+20.0

M_{nTh} = theoretical M_n.
[a] Commercial amorphous PLA.
[b] Calculated from ^{1}H NMR results.
[c] HPSEC-MALLS-dRI in THF, 0.5 min.
[d] Determined by DSC.
[e] Obtained from literature [41].

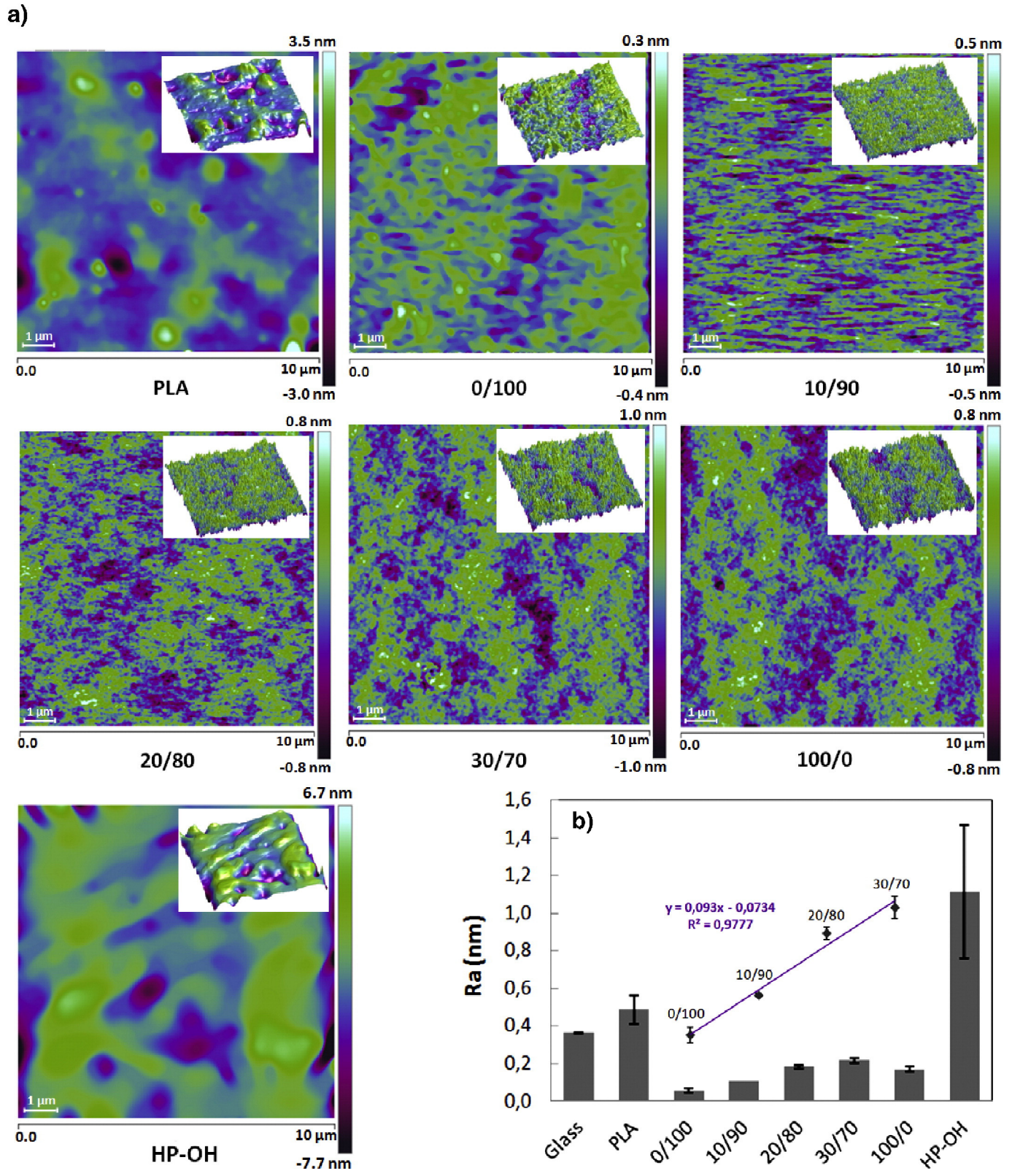

Fig. 4. Polymers AFM: (a) 2D and 3D images and (b) average roughness Ra (nm) and Ra linear correlation with % A of polymers.

basic component of the surface energy is very small for all the samples and statistically significantly different ($p < 0.001$ for all groups), two by two (10/90—20/80, 20/80—30/70, 30/70—100/0 and 100/0—HP-OH), using n = 20 different values for each group. No significant difference ($p > 0.05$) between groups (PLA—0/100, 0/100—10/90) was observed. In addition, the non-corrected acidic components (Fig. 5b) are related to AP and statistically significantly different, two by two (0/100—10/90, 10/90—20/80, 20/80—30/70, 30/70—100/0 and 100/0—HP-OH) using n = 20 different values for each group ($p < 0.001$ for all groups) except for PLA—0/100 group ($p > 0.05$).

Table 3
Water, formamide and diiodomethane contact angles by sessile drop method for all the surfaces.

Samples	Glass	PLA	0/100	10/90	20/80	30/70	100/0	HP-OH
Water contact angle (°)	39.24 ± 0.80	77.28 ± 0.58	92.44 ± 0.36	88.73 ± 0.61	85.94 ± 0.09	81.10 ± 0.88	25.68 ± 1.35	72.15 ± 0.18
Formamide contact angle (°)	30.04 ± 1.47	37.45 ± 1.05	66.44 ± 0.08	71.76 ± 0.74	76.65 ± 0.14	78.21 ± 0.47	21.96 ± 1.07	22.11 ± 0.80
Diiodomethane contact angle (°)	44.6 ± 1.18	25.34 ± 1.70	41.42 ± 0.01	42.69 ± 0.04	45.25 ± 0.50	47.25 ± 0.49	53.13 ± 1.50	43.35 ± 1.04

All of the above data of PLA sample were in accordance with the reported studies in the literature [46].

3.3. Cassie corrections of contact angles and surface energies

Fig. 6a details the linear fit of relationship between the Cassie corrected surface energy and components versus the Cassie corrected water contact angle for the two references samples and the three copolymers. These five samples range from 0 to 100% of AP with the references located at the extremes. All the energy components are found to be different significantly, two by two ($p < 0.01$), except 0/100 compared to 10/90 for basic component because of very small values.

All the energies, except the LW component, decrease when contact angle increases (surface more and more hydrophobic). Fig. 6b shows the reverse behavior versus AP.

However, little discrepancies were observed between the two representations and this was quantified by the values of R^2 correlation coefficient (linear fit extrapolation) in all the cases (Fig. 7). The linear fits were compared for corrected (*) or non-corrected contact angles and energy values in versus contact angle or AP. The basic component is the one that needs to be corrected the most.

It was worth noting that if Cassie correction is applied, representations versus contact angles or versus AP bring both R^2 values closer to 1 than if not corrected (Fig. 7). After correction it was observed that R^2 for contact angle was higher than for AP whereas it is the reverse if no correction is made. In case it is impossible to apply Cassie correction, it is better to represent the relationship between surface energy and components versus AP than versus water contact angle.

In order to go further on the evaluation of the impact of Cassie correction on contact angles (Fig. 8a) and on surface energies (Fig. 8b) relative percentage of the correction was calculated as a function of AP. Relative impact of Cassie correction is maximum for formamide first (maximum 28%). then water (6% maximum) and finally diiodomethane. This result can be explained by the fact that formamide and water are polar solvents compared to diiodomethane. The necessity for correction increases with AP.

Moreover, total and acid energy components relative corrections (%) increase with AP whereas base and acid–base ones diminish. Corrections could reach 100% for basic component around 80% for acid–base one and around 50% for acidic surface energy.

It is important to quantify Polar acid–base and/or apolar surface energy components with accuracy for a better understanding of cell behavior in contact with a biomaterial [27]. Indeed, water contact angle and total surface free energy are generally not sufficient parameters to explain differences in cell response. In contrast, acidic or basic surface energy components can be parameters but enable us to discriminate

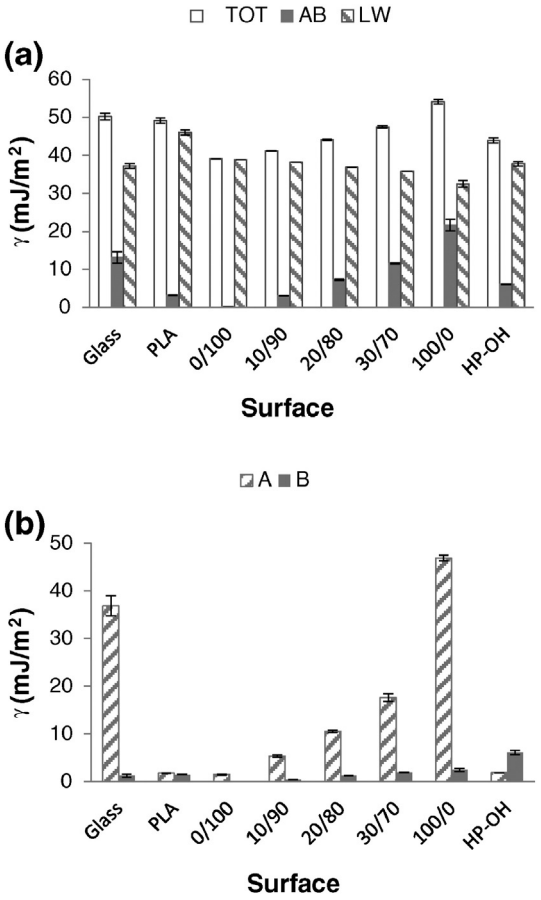

Fig. 5. (a) Total surface free energy (γTOT) dispersive (LW) and polar acid–base (AB). (b) Acidic and basic components of surface energy for each surface.

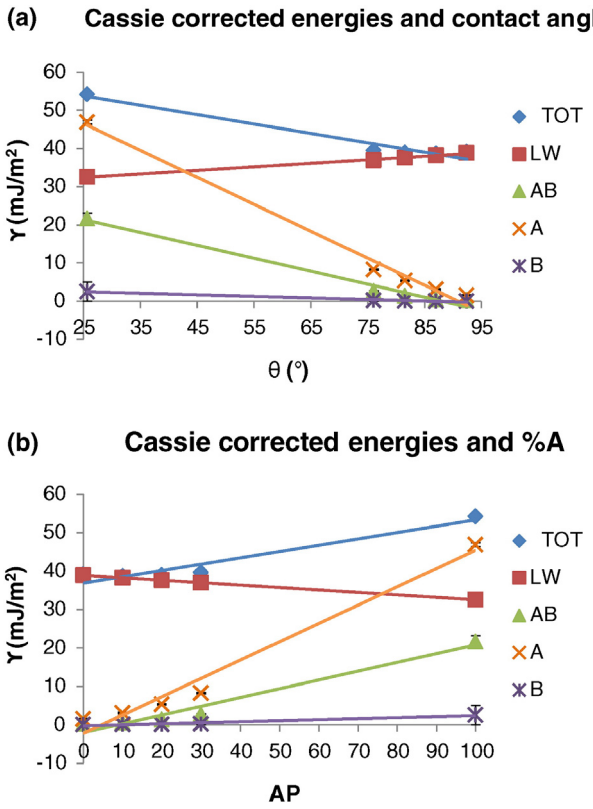

Fig. 6. Surface free energy and components versus water contact angle after Cassie correction (a) versus θ and (b) versus % A.

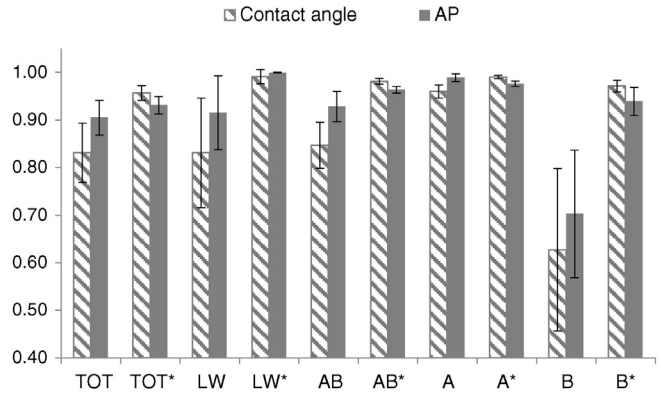

Fig. 7. Linear correlation coefficient R^2 as a function of water contact angle or AP for surface energy components.

between biomaterial surfaces [27]. That is why it is of importance, in biomaterial research, not only to reach these values but also to correct them from artifacts such as those induced by the different chemical composition of polymers structure. Besides, an analysis of protein adsorption onto the surfaces of interest could help to go further in the understanding of the correlations between material surface chemistry and biocompatibility. For example, dynamic contact angle (DCA) could detect particular protein adsorption behavior depending on the biomaterial surface chemistry as it has been shown for polysaccharides polyelectrolytes films. In this study, endothelial cell proliferation was found to be in relation with the ability of fibronectin to easily change the conformation during DCA cycling depending on the film surface chemistry [21].

Biocompatibility, mechanical properties, and drug-loading capacity are the general considerations of a selected polymer as stent-coating for eluting drugs. Indeed, the surface properties of the polymer which covers the stent are the main factor that affects the biological response (immediate and long-term response) between the stent and the vascular tissue and blood. These stent-coating surface properties are the surface texture, charge and energy. According to literature, the surface energy is the most important factor in determining the thrombogenicity in blood. The affinity of the polymer surface with water increases with increasing surface energy and therefore the increase of thrombogenicity in the blood medium [48].

Another very important factor is the surface roughness. The thrombogenicity increases on rougher surfaces. This due to the higher blood protein adsorption, activation and aggregation of platelet [48]. Thus, a stent coating should have good interaction with blood, be incorporated by the vascular tissue and present the advantage to minimize the inflammatory response. This is thanks to its good surface properties.

The present work shows that this biomaterial presents good thermal and surface properties (low *Tg* and surface energy and functional hydrophilic molecules on its chain which adjusts their properties and interactions with body tissue). This precisely meets the requirements of the intended cardiovascular application.

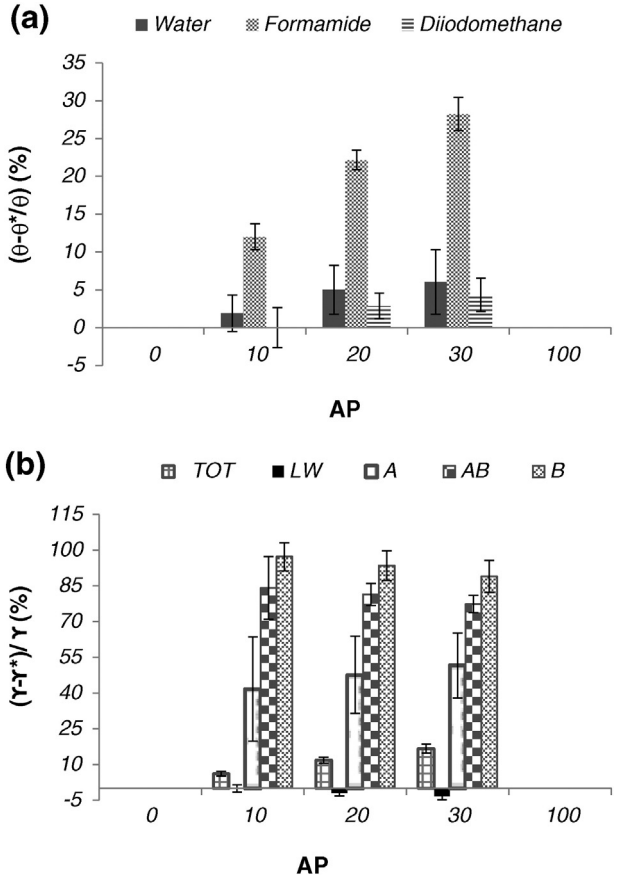

Fig. 8. (a) Impact of Cassie–Baxter correction on contact angle versus AP for water formamide and diiodomethane probe liquids. (b) Relative modification of surface energy values after Cassie–Baxter correction.

4. Conclusion

In this work, the wettability of the different PDMMLA derivatives' surfaces was successfully characterized. On the one hand, the surface free energy and its components (dispersive, polar, acid and basic) were determined for each surface. On the other hand, influence of acidic percentage incorporated in the side-chain of copolymers on wettability, morphology and surfaces properties of polyesters was investigated because three of these samples exhibited a heterogeneous chemical composition. Cassie–Baxter equation was used to bring corrections to the experimental contact angles. Finally, the impact of this correction on contact angles and subsequent surface energy and components was quantified. It was found necessary to apply correction in order to improve the quality of the relationships obtained between the wettability parameters and the percentage of acid indicated in the chemical formula of the polymer. Moreover, as shown in this study, adding only 10% of acidic hydrophilic group in a polymer chemical composition, allows us not only to shape rational design structure and the morphology of the PDMMLA copolymers, but also to control and tailor their wettability properties. This approach that focuses on their thermomechanical properties is important to study their degradation rate and their biological effects considering that hydrophilic/hydrophobic balance plays an important role in the material/cell's interactions.

References

[1] H.Y. Tian, Z.H. Tang, X.L. Zhuang, X.S. Chen, X.B. Jing, Biodegradable synthetic polymers: preparation, functionalization and biomedical application, Progress In Polymer Science 37 (2011) 237–280.
[2] K.F.D.W. Pack, A.M. Klibanov, R. Langer, Visual evidence of acidic environment within degrading poly(lactic-co-glycolic acid) (PLGA) microspheres, Pharmaceutical Research 17 (2000) 100–106.
[3] R. De Santis, A. Russo, A. Gloria, U. D'Amora, T. Russo, S. Panseri, M. Sandri, A. Tampieri, M. Marcacci, V.A. Dediu, C.J. Wilde, L. Ambrosio, Towards the design of 3D fiber-deposited poly(epsilon-caprolactone)/iron-doped hydroxyapatite nanocomposite magnetic scaffolds for bone regeneration, Journal Of Biomedical Nanotechnology 11 (2015) 1236–1246.
[4] Z.W. Huang, V. Laurent, G. Chetouani, J.Y. Ljubimov, E. Holler, T. Benvegnu, P. Loyer, S. Cammas-Marion, New functional degradable and bio-compatible nanoparticles based on poly(malic acid) derivatives for site-specific anti-cancer drug delivery, International Journal Of Pharmaceutics 423 (2012) 84–92.
[5] J.Y. Ljubimova, J. Portilla-Arias, R. Patil, H. Ding, S. Inoue, J.L. Markman, A. Rekechenetskiy, B. Konda, P.R. Gangalum, A. Chesnokova, A.V. Ljubimov, K.L. Black, E. Holler, Toxicity and efficacy evaluation of multiple targeted polymalic acid conjugates for triple-negative breast cancer treatment. Journal of Drug Targeting 21 (2013) 956–967.

[6] P. Loyer, S. Cammas-Marion, Natural and synthetic poly(malic acid)-based derivates: a family of versatile biopolymers for the design of drug nanocarriers. Journal of Drug Targeting 22 (2014) 556–575.
[7] A. Lanz-Landázuri, A. Martínez de Ilarduya, M. García-Alvarez, S.n. Muñoz-Guerra, Poly(β,L-malic acid)/doxorubicin ionic complex: a pH-dependent delivery system, Reactive and Functional Polymers 81 (2014) 45.
[8] Y. Qiao, X. Duan, L. Fan, W. Li, H. Wu, Y. Wang, Synthesis of controlled molecular weight poly (β-malic acid) and conjugation with HCPT as a polymeric drug carrier, Journal of Polymer Research 21 (2014) 1–9.
[9] P. McDonald, J. Lyons, L. Geever, C. Higginbotham, In vitro degradation and drug release from polymer blends based on poly(dl-lactide). poly(l-lactide-glycolide) and poly(ε-caprolactone), Journal of Materials Science 45 (2009) 1284–1292.
[10] S.T. Schmitz-Hertzberg, W.C. Mak, K.K. Lai, C. Teller, F.F. Bier, Multifactorial design of poly(d.l-lactic-co-glycolic acid) capsules with various release properties for differently sized filling agents, Journal of Applied Polymer Science 130 (2013) 4219.
[11] L. Wang, X. Jia, Y. Chen, Y. Che, Z. Yuan, Synthesis, degradability, and cell affinity of poly (DL-lactide-co-RS-hydroxyethyl-beta-malolactonate), Journal Of Biomedical Materials Research Part A 87A (2008) 459–469.
[12] K.L. Lai, B. He, Z.W. Gu, Preparation and cell compatibility of functionalized biodegradable poly(DL-lactide-co-RS-beta-malic acid), Chinese Journal Of Polymer Science 26 (2008) 177–186.
[13] Y. Liu, W. Wang, J. Wang, Y. Wang, Z. Yuan, S. Tang, M. Liu, H. Tang, Blood compatibility evaluation of poly(d.l-lactide-co-beta-malic acid) modified with the GRGDS sequence, Colloids and Surfaces B: Biointerfaces 75 (2010) 370.
[14] J. Qian, W. Xu, W. Zhang, X. Jin, Preparation and characterization of biomorphic poly(l-lactide-co-β-malic acid) scaffolds, Materials Letters 124 (2014) 313.
[15] Y. Zhang, C. Ni, G. Shi, J. Wang, M. Zhang, W. Li, The polyion complex nano-prodrug of doxorubicin (DOX) with poly(lactic acid-co-malic acid)-block-polyethylene glycol: preparation and drug controlled release, Medicinal Chemistry Research 24 (2015) 1189–1195.
[16] H. Ding, G. Helguera, J.A. Rodriguez, J. Markman, R. Luria-Perez, P. Gangalum, J. Portilla-Arias, S. Inoue, T.R. Daniels-Wells, K. Black, E. Holler, M.L. Penichet, J.Y. Ljubimova, Polymalic acid nanobioconjugate for simultaneous immunostimulation and inhibition of tumor growth in HER2/neu-positive breast cancer, Journal of Controlled Release 171 (2013) 322–329.
[17] B.-S. Lee, M. Vert, E. Holler, Water-soluble Aliphatic Polyesters: Poly(Malic Acid)s, Biopolymers Online. Wiley-VCH Verlag GmbH & Co, KGaA, 2005.
[18] B. Gasslmaier, et al., Synthetic substrates and inhibitors of β-poly(L-malate)-hydrolase (polymalatase), Eur. J. Biochem. 267 (2000) 5101.
[19] B. He, J. Bei, S. Wang, Morphology and degradation of biodegradable poly(L-lactide-co-β-malic acid), Polymers for Advanced Technologies. 14 (2003) 645–652.
[20] L.K. Sarah, X.T. Vinh, K. Cathrin, P.B. Anaïs, P.D. Andrew, Synthetic strategies, sustainability and biological applications of malic acid-based polymers, Green Materials 2 (2014) 107–122.
[21] S. Benni, T. Avramoglou, H. Hlawaty, L. Mora, Dynamic contact angle analysis of protein adsorption on polysaccharide multilayer's films for biomaterial reendothelialization, BioMed research international 2014 (2014) 679031.
[22] D. Bonn, J. Eggers, J. Indekeu, J. Meunier, E. Rolley, Wetting and spreading, Reviews Of Modern Physics 81 (2009) 739–805.
[23] E.H. Sohn, B.G. Kim, J.S. Chung, H. Kang, J.C. Lee, Wettability of the morphologically and compositionally varied surfaces prepared from blends of well ordered comb-like polymer and polystyrene, Journal of Colloid and Interface Science 354 (2011) 650.
[24] T.T. Chau, W.J. Bruckard, P.T.L. Koh, A.V. Nguyen, A review of factors that affect contact angle and implications for flotation practice, Advances In Colloid And Interface Science 150 (2009) 106–115.
[25] R. Di Mundo, F. Bottiglione, G. Carbone, Cassie state robustness of plasma generated randomly nano-rough surfaces, Applied Surface Science 316 (2014) 324–332.
[26] E. Bormashenko, Why does the Cassie–Baxter equation apply? Colloids And Surfaces A-Physicochemical And Engineering Aspects 324 (2008) 47–50.
[27] L. Ponsonnet, K. Reybier, N. Jaffrezic, V. Comte, C. Lagneau, M. Lissac, C. Martelet, Relationship between surface properties (roughness. wettability) of titanium and titanium alloys and cell behaviour, Materials Science & Engineering C-Biomimetic And Supramolecular Systems 23 (2003) 551–560.
[28] C. Barbaud, S. Cammas-Marion, P. Guerin, Poly(beta-malic acid) derivatives with non-charged hydrophilic lateral groups: synthesis and characterization, Polymer Bulletin 43 (1999) 297–304.
[29] C. Barbaud, F. Faÿ, F. Abdillah, S. Randriamahefa, P. Guérin, Synthesis of new homopolyester and copolyesters by anionic ring-opening polymerization of α,α′,β-trisubstituted β-lactones, Macromolecular Chemistry and Physics 205 (2004) 199.
[30] F. Ouhib, S. Randriamahefa, P. Guerin, C. Barbaud, Synthesis of new statistical and block co-polyesters by ROP of alpha,alpha,beta-trisubstituted beta-lactones and their characterizations, Designed Monomers And Polymers 8 (2005) 25–35.
[31] C. Barbaud, F. Abdillah, F. Faÿ, M. Guerrouache, P. Guérin, Synthesis of new alpha,alpha,beta-trisubstituted beta-lactones as monomers for hydrolyzable polyesters, Designed Monomers and Polymers 6 (2003) 353.
[32] F.E. Kohn, et al., The ring-opening polymerization of D,L-lactide in the melt initiated with tetraphenyltin, Journal Of Applied Polymer Science 29 (1984) 4265–4277.
[33] J. Van Oss Carel, Forces interfaciales en milieux aqueux. Chimie(ed. Masson) 1996 14–402.
[34] Y. Huang, H.C.A. Ng, X.W. Ng, V. Subbu, Drug-eluting biostable and erodible stents, Journal of Controlled Release 193 (2014) 188.
[35] F.M. Zambaux, F. Bonneaux, R. Gref, E. Dellacherie, C. Vigneron, MPEO-PLA Nanoparticles: Effect of MPEO Content on Some of Their Surface Properties, 44John Wiley & Sons. Inc., 1999 109–115.
[36] L. Xiao, et al., Poly(Lactic Acid)-Based Biomaterials: Synthesis, Modification and Applications. Chapter 11, INTECH Open Access Publisher, 2012 248–282.
[37] M. Persson, et al., Effect of bioactive extruded PLA/HA composite films on focal adhesion formation of preosteoblastic cells, Colloids Surf. B: Biointerfaces 121 (2014) 409.
[38] Y.-Q. Wang, J.-Y. Cai, Enhanced cell affinity of poly(l-lactic acid) modified by base hydrolysis: wettability and surface roughness at nanometer scale, Curr. Appl. Phys. 1 (2007) 108.
[39] I.M. De Rosa, et al., Poly(lactic acid)/phormium tenax composites: morphology and thermo-mechanical behavior, Polym. Compos. 32 (2011) 1362.
[40] J. Wang, et al., Preparation and pH controlled release of polyelectrolyte complex of poly(l-malic acid-co-d,l-lactic acid) and chitosan, Colloids Surf. B: Biointerfaces 115 (2014) 275.
[41] M.A. LeboucherDurand, V. Langlois, P. Guerin, 4-carboxy-2-oxetanone as a new chiral precursor in the preparation of functionalized racemic or optically active poly(malic acid) derivatives, Polym. Bull. 36 (1996) 35–41.
[42] S. Cammas, M.M. Bear, L. Moine, R. Escalup, G. Ponchel, K. Kataoka, P. Guerin, Polymers of malic acid and 3-alkylmalic acid as synthetic PHAs in the design of biocompatible hydrolyzable devices, International Journal of Biological Macromolecules 25 (1999) 273–282.
[43] Gaydos, A.W. Neumann, Line tension in multiphase equilibrium systems, Applied Surface Thermodynamics (1996) 169–238.
[44] E.I. Vargha-Butler, E. Kiss, C.N.C. Lam, Z. Keresztes, E. Kalman, L. Zhang, A.W. Neumann, Wettability of biodegradable surfaces, Colloid And Polymer Science 279 (2001) 1160–1168.
[45] D. Cohn, H. Younes, Biodegradable PEO/PLA block copolymers, Journal of Biomedical Materials Research 22 (1988) 993.
[46] Spiridon, K. Leluk, A.M. Resmerita, R.N. Darie, Evaluation of PLA-lignin bioplastics properties before and after accelerated weathering, Composites Part B-Engineering 69 (2015) 342–349.
[47] I. Chemistry, Operating manual DataPhysics OCA, DataPhysics Instruments GmbH, 1–4, 2002.
[48] Y. Huang, Drug Eluting Stents: Anti-inflammatory Approach to Prevent Restenosis After Stent Implantation, 2003.